Exponential and power-law mass distributions in brittle fragmentation

J. A. Åström
Center for Scientific Computing, P. O. Box 405, FIN-02101 Esbo, Finland

R. P. Linna
Department of Physics, University of Jyväskylä, P. O. Box 35, FIN-40351 Jyväskylä, Finland
and Laboratory of Physics, Helsinki University of Technology, P.O. Box 1100, FIN-02015 HUT, Finland

J. Timonen
Department of Physics, University of Jyväskylä, P. O. Box 35, FIN-40351 Jyväskylä, Finland

Peder Friis Møller and Lene Oddershede
The Niels Bohr Institute, Blegdamsvej 17, DK-2100 Copenhagen Ø, Denmark
(Received 7 January 2004; published 11 August 2004)

Generic arguments, a minimal numerical model, and fragmentation experiments with gypsum disk are used to investigate the fragment-size distribution that results from dynamic brittle fragmentation. Fragmentation is initiated by random nucleation of cracks due to material inhomogeneities, and its dynamics are pictured as a process of propagating cracks that are unstable against side-branch formation. The initial cracks and side branches both merge mutually to form fragments. The side branches have a finite penetration depth as a result of inherent damping. Generic arguments imply that close to the minimum strain (or impact energy) required for fragmentation, the number of fragments of size s scales as $s^{-(2D-1)/D} f_1(-(2/\lambda)^D s) + f_2(-s_0^{-1}(\lambda + s^{1/D})^D)$, where D is the Euclidean dimension of the space, λ is the penetration depth, and f_1 and f_2 can be approximated by exponential functions. Simulation results and experiments can both be described by this theoretical fragment-size distribution. The typical largest fragment size s_0 was found to diverge at the minimum strain required for fragmentation as it is inversely related to the density of initially formed cracks. Our results also indicate that scaling of s_0 close to this divergence depends on, e.g., loading conditions, and thus is not universal. At the same time, the density of fragment surface vanishes as L^{-1}, L being the linear dimension of the brittle solid. The results obtained provide an explanation as to why the fragment-size distributions found in nature can have two components, an exponential as well as a power-law component, with varying relative weights.

DOI: 10.1103/PhysRevE.70.026104 PACS number(s): 46.50.+a, 62.20.Mk

I. INTRODUCTION

Fragmentation is a fundamental process in nature. An example of microscopic fragmentation is nuclear fission, while soil particles, sand, boulders, and meteorites are fragments on scales that range from micrometers to meters, respectively. Asteroids and tectonic plates are still larger fragments, while supernovas serve as an example of a violent fragmentation process on an astronomical scale.

During the last few years, there has emerged evidence of a continuous (or weakly discontinuous) transition between a damaged and a fragmented state in numerical models of brittle solids [1–3]. When elastic energy is fed into a solid, this will be either fragmented or merely damaged depending mainly on the amount of energy provided. Here, fragmentation means that the mass fraction of the largest fragment vanishes for large systems, while a damaged state means that the mass of the largest "fragment" is almost proportional to L^D, where L is the linear dimension of the solid and D its Euclidean dimension. At the point of minimum energy needed to fragment the solid, the distribution of fragment sizes may become scale invariant, $n(s)ds \propto s^{-\alpha}$. At this transition point, the average density of fracture surface should, for a large solid, vanish continuously as the damaged state is approached from the fragmented state by decreasing the energy.

During the last two decades, similar observations have been made of the fragmentation of heavy nuclei. The first power-law-like fragment-size distributions resulting from experiments on heavy nuclei were discovered in the early 1980's [4,5]. It was suggested that the origin of these results is a percolation type of bond breaking between nucleons, which leads to fragmentation [6,7] ($\alpha \approx 2.35$), and a model based on statistical multifragmentation was later found to describe the experimental mass distributions for a wide range of impact energies [8].

Within the mining engineering community, an empirical scale-invariant fragment-size distribution has long been known as the Gaudin–Schuhmann distribution [9,10] (or the Gates–Gaudin–Schuhmann distribution). According to this distribution, the total mass of fragments with an effective radius smaller than r, scales over a few orders of magnitude in the small-fragment limit as r^γ with $\gamma \approx 1$ ($\alpha = 5/3$ for $D = 3$).

There is thus a considerable amount of indications that fragment-size distributions can become scale invariant. However, there seems to be little or no consistency in the values found for the scaling exponents. For example, these exponents seem to depend on whether the considered fragmenta-

tion is a grinding type of process [11] ($\alpha=1.0-2.0$), a collision [2] ($\alpha\approx 2.3$), or an expansive explosion [3] ($\alpha=1.5$). The scaling exponent may also depend on the impact energy [12] and on the shape of the fractured object [13]. In the case of nuclear fragmentation, the exponent of the power-law depends, e.g., on temperature [14] and impact energy [8]. In the experimental Gaudin–Schuhmann distributions, the exponent of the power law also varies even though it is always fairly close to unity [15]. Furthermore, there are experimental fragment-size distributions that do not have a scale invariant contribution at all, and the distribution is described by an exponential function [16]. A slow grinding type of fragmentation processes (like in the formation of soils) typically result in log–normal fragment-size distributions, but such processes are not considered here.

It is quite obvious that fragmentation processes depend strongly, e.g., on boundary effects and loading conditions. Loading conditions in particular are important as there are at least two basic fragmentation mechanisms in operation. One is the early-stage cracking of the solid, and the other is the breaking of already existing fragments in collisions with other fragments. Furthermore, material properties like elasticity, plasticity, and/or viscoelasticity, certainly affect fragmentation. Also, temperature fluctuations and quenched disorder versus stress concentration at the crack tips strongly affect crack propagation, and thereby the outcome of fragmentation. In order to look for possible universal features inherent to the fragmentation processes, it is thus important to construct as minimal a model as possible for fragmentation. The purpose of this article is to present such a minimal model, which leads to some analytical predictions, and then to complement these predictions and to test the validity of this model by numerical simulations and real experiments.

II. ANALYTICAL MODEL

In our model, we consider the application of a scalar strain field to an elastic material, which results in the development of a stress field $\tau(\boldsymbol{x},t)$. When the maximum local loading in a sample reaches the failure threshold of the material, a crack will be nucleated. In a brittle material, this nucleation leads to crack propagation unless the disorder in the material is too strong so as to cause stress fluctuations to dominate over stress concentration at the crack tip.

Cracks have an effective attractive interaction. This means that a crack propagating alongside an already existing crack will turn toward this crack, and eventually "die" by terminating (at an almost right angle) at the free fracture surface left behind by it. Thus, propagating cracks will begin to form fragments. We consider here brittle materials in which material strength/stiffness variations are uncorrelated. The cracks nucleated in this kind of material, after it has been homogeneously strained beyond the point where the first crack is nucleated, will thus appear in uncorrelated positions. The fragment-size distribution resulting from mergings of these cracks will be an exponential function [17]. The typical fragment size in such a Poisson process can be written as $s_0 \propto \rho^{-1}$, where ρ is the density of the nucleated cracks [compare the highly stretched sheet in Fig. 1(A) to the slightly less stretched sheet in Fig. 1(B)].

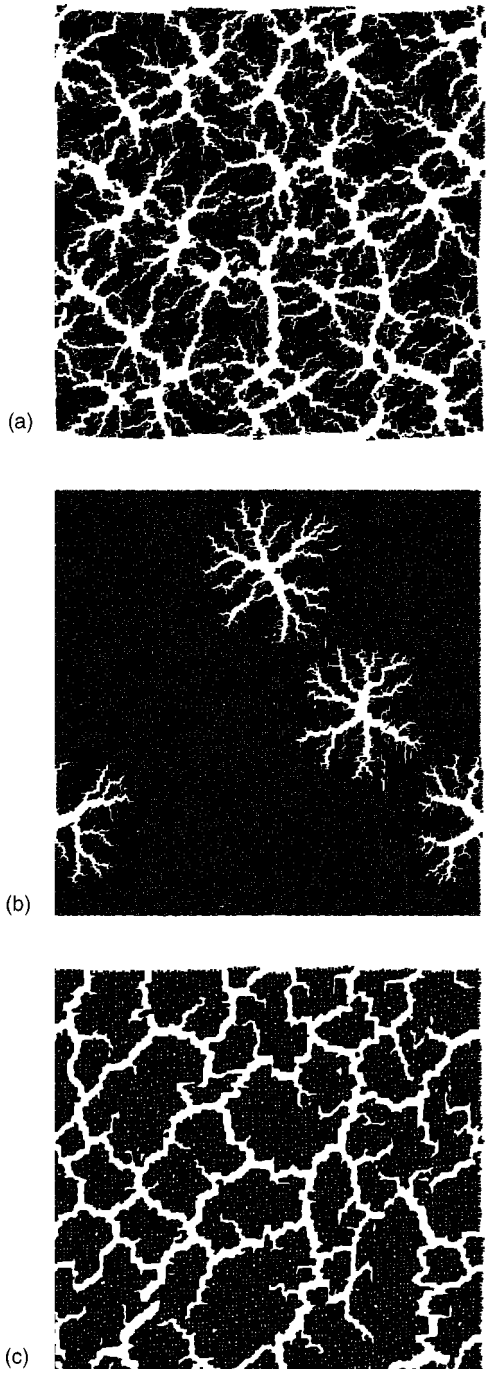

FIG. 1. Snapshots of simulation of fragmentation of brittle sheets. In (A) $\sigma=0.016$, $c=0.001$, in (B) $\sigma=0.026$, $c=0.001$, and in (C) $\sigma=0.016$, $c=1.0$. $L=240$.

As the elastic energy loaded in the sample by the time nucleation of cracks begins is typically high in comparison with the energy released in the formation of a fracture surface, the nucleated cracks will propagate very fast and be unstable against branching or bifurcation (or crack-tip splitting) [18]. All propagating cracks will thus emit side branches, and adjacent side branches will attract each others exactly as neighboring cracks do. Thus, neighboring side branches around a propagating crack will eventually merge so as to form small-size fragments [19–21]. When the tip of

a side branch is merged with an adjacent free fracture surface, it creates a "merging point" beyond which only one branch (a "second-generation" branch) appears to propagate. Since adjacent "first-generation" branches have a well-defined average mutual distance [22] l_b, we can estimate the fragment-size distribution that results from this kind of merging process by using a simplified model in which all adjacent side branches are separated by l_b.

If n_b branches at intervals l_b are formed around a propagating crack, then in the first generation of mergings $n_b/(2^{D-1})$ fragments of typical size l_b^D will be formed. Every other branch (on the average) has thereby disappeared so that the (average) distance between the remaining (second-generation) branches is $2l_b$. These branches attract each others, and adjacent ones of them eventually merge to form $n_b/(4^{D-1})$ fragments of typical size $(2l_b)^D$, whereby again half of the remaining branches are removed. If this process is continued, it can easily be shown to produce a fragment-size distribution

$$n(s)ds \propto s^{-(2D-1)/D}. \tag{1}$$

Notice that the only assumptions needed for this result are that the crack instabilities appear at intervals which can be characterized by a typical length scale [22] (i.e., scale-invariant distributions are not allowed), and that the fragments formed have an aspect ratio independent of size. The derivation of Eq. (1) also involves the assumption that the fragmentation process is heterogeneous enough to produce a continuous distribution. Equation (1) has been reported before [24,21,23], but as a result of quite different arguments.

Equation (1) is equivalent to the empirical Gaudin–Schuhmann (GS) distribution: $N_g(r)=\int_0^r r^D n(r)dr$, with $r \propto s^{1/D}$, gives $N_g(r) \propto r$, which is the GS distribution. Equation (1) is also consistent with several numerical studies of fragmentation [1,19,21,25], and with the recent two-dimensional experimental results reported in Refs. [26,27]. In Refs. [13,24], experimental results are reported for both two- and three-dimensional fragmentation. From these two sets of results, the three-dimensional ones are consistent with Eq. (1), while the two-dimensional ones are not ($\alpha \approx 1.2$). This inconsistency may depend, e.g., on loading conditions as demonstrated in Ref. [28]. In any case, it is clear that the size distribution of fragments obey Eq. (1) in the small-fragment regime for a large class of brittle fragmentation.

Mechanisms that also need to be taken into account include energy dissipation in the branching and bifurcation processes, and the elastic relaxation of the existing fragments. These mechanisms lead to a finite penetration depth for the crack branches away from their parent cracks [compare Figs. 1(A) and 1(C)] so that there will be a cutoff in the power-law distribution Eq. (1), expected still to be valid for small fragment sizes.

The fragment-size distribution that results from merging side branches can thus be expressed in the general form

$$n(s) \propto s^{-\alpha} f_1(s/s_1) \tag{2}$$

with $\alpha=(2D-1)/D$ as before. The "scaling function" f_1 should be independent of s for fragments much smaller than

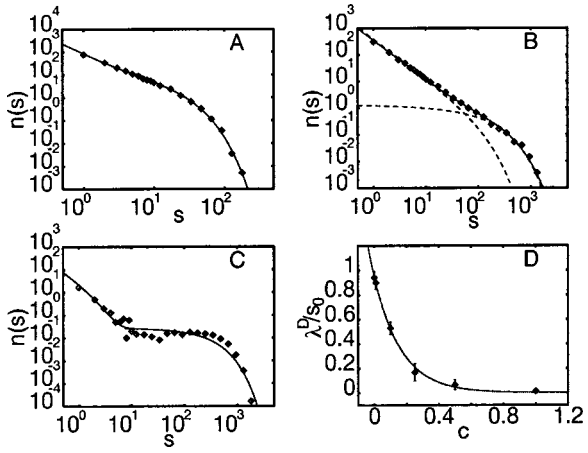

FIG. 2. $n(s)$ for disorder type I with (**A**) $\sigma=0.018$ and (**B**) $\sigma=0.025$. The numerical distributions are fitted by Eq. (3). In (**A**) $s_0=32.5$ and in (**B**) $s_0=460$. The number of free parameters is reduced by using $\lambda^D=s_0$. The two terms of Eq. (3) are also shown separately in (**B**). (**C**) is the same case as in (**A**) but with a large damping coefficient $c=1.0$. In this case, $s_0=430$ and $\lambda=4.0$. (**D**) shows λ^D/s_0 as a function of c. Simulation data are compared to the exponential function $\lambda^D/s_0=\exp(-c/\text{constant})$.

s_1, and decay rapidly for $s>s_1$. The penetration depth is then $\lambda \sim (s_1)^{1/D}$. For simplicity, we will assume in the following that f_1 is an exponential function.

The sizes of the Poisson-process fragments will be reduced by the creation of small-size fragments around each crack by the side-branch-merging process described above, such that the total fragment-size distribution can finally be approximated by a superposition of two distribution functions,

$$n(s) \propto (1-\beta_r)s^{-\alpha}\exp(-(2/\lambda)^D s)+\beta_r \exp(-s_0^{-1}(s^{\frac{1}{D}}+\lambda)^D), \tag{3}$$

where $s^{1/D}+\lambda$ is the reduced linear size of the Poisson-process fragments and β_r determines the relative normalization of the two parts of the distribution. To demonstrate the role of the two terms in Eq. (3), they are shown separately in Fig. 2(B) together with the full distribution. From Fig. 2(B), it is evident how β_r must be chosen according to the relative weight of small and large fragments. The locations of the two cutoffs, λ and s_0, are also clearly seen in this figure. In Fig. 2(C), the separation of the distribution into two terms is evident even without plotting the terms separately.

For a homogeneous strain in $D=1$, fragmentation is simply random cutting of a line. Branches cannot be formed and, trivially, $\beta_r=1$ and $\lambda=0$. Equation. (3) becomes now a pure exponential function as it should for a one-dimensional Poisson process.

For $D>1$, there appear nontrivial cases: When $\lambda \to s_0^{1/D}$, the residual (exponential) part almost vanishes, and if furthermore the strain becomes so low that the density of the nucleated cracks begins to vanish, $n(s)$ becomes a pure power law. In the limiting case, the fragments are formed by mergings of the branches of a single nucleated crack, with the small fragments near the main crack and larger fragments

farther away. This is the transition point from a fragmented to a merely damaged sample. In a sample of size L^D, the number of fragments of any size should scale as L^{D-1}. The size of the largest fragment should scale as L^D. The average density of fracture surface should thus scale as L^{-1}, if the localized microcracks are excluded.

To test Eq. (3), we use here a minimal numerical model in $D=2$, and in $D=3$ the results of impact fragmentation of gypsum disks. The experimental results reported here complement those of large-scale quarry blastings of granitic gneiss, which have been reported elsewhere [29].

III. NUMERICAL MODEL

In order to test Eq. (3) in $D=2$, we constructed a minimal numerical model of a brittle solid. To begin with, some kind of discretization of the system is needed. For an investigation of universal features in the fragmentation of brittle materials, there is no need to specifically model any particular material. Therefore, we use here a standard model of a solid, which describes it as a lattice of discrete mass points connected by elastic and breakable beams. We use a square lattice that obviously suffers from anisotropy, but whose disorder is easily controllable, contrary to those in isotropic grid structures such as, e.g., Voronoi lattices. A beam-lattice model fulfills rotational invariance, which is important when modeling fragmentation.

In a minimal model, there is no strain or strain-rate dependence in the local stiffness constants, and fracture should be instantaneous and irreversible in contrast with models that allow gradual softening and healing. We use linear elastic beams that simply vanish once a fracture threshold is exceeded. The simplest possible threshold is a deformation threshold independent of the deformation direction (i.e., a beam vanishes when $\delta l/l > \sigma$, where δl is the magnitude of the relative displacement difference between the end points of the beam, and σ the fracture threshold).

We use periodic boundary conditions, and loading is performed by expanding the periodic box up to a maximum strain ϵ_m [$\epsilon(t)=\epsilon_m \sin^2(\omega t)$, for $t \leqslant \pi/(2\omega)$, $\epsilon(t)=\epsilon_m$, otherwise]. In the discrete Newton's equations of motion for the system it is easy to remove the inertial effects related to the expansion of the periodic box. The inertia created in the elastic relaxation of the system (now a sheet in $D=2$) is damped by a "viscous" damping force ($F_d=-c\dot{x}$) in the equations of motion. Fragmentation is allowed only after the maximum strain is reached. Thereafter, the fracture criterion is checked for every beam at every time step in the simulation of the dynamics.

The features of the minimal model described above are rather intuitive. A nontrivial aspect of the problem is how to include the random uncorrelated variations in the properties of the material. If a perfectly homogeneous lattice is strained using a scalar tensile strain field, and the lattice has no boundaries, then all bonds will reach the fracture threshold at the same time and vanish instantaneously, which of course is not desirable. In a square, lattice cracks and branches will preferably propagate in the "soft" directions of the lattice. In order to avoid the first and to diminish the second effect, we introduce random fluctuations in the system by geometrically distorting the lattice sites as, e.g., in Ref. [3]. A distortion parameter δ_1 takes values between 0 and 1, where 0 corresponds to zero distortion and 1 to maximum distortion. In order to mimic disorder commonly present in brittle materials, we also use uniformly distributed uncorrelated variations in the Young's modulus E of the beams ($E \in [1-\delta_2, 1+\delta_2]$), and introduce a small fraction (δ_3) of prebroken bonds to model microcracks. We concentrate on two cases: (I) $\delta_1=0.7$, $\delta_2=0.0$, $\delta_3=0.0$, and (II) $\delta_1=0.3$, $\delta_2=0.1$, $\delta_3=0.001$. Some other types of disorder were also tested without any significant changes in the results. We have not attempted a systematic investigation of different types of disorder, however.

IV. NUMERICAL RESULTS

Figure 1 shows samples of fragmented sheets for disorder parameters $\delta_1=0.7$, $\delta_2=0.0$, $\delta_3=0.002$. The fracture threshold is $\sigma=0.016$ in Fig. 1(A) and $\sigma=0.026$ in Fig. 1(B). In both these cases $c=0.001$. In Fig. 1(C) $\sigma=0.016$ and $c=1.0$. The maximum strain is $\epsilon_m=0.01$. The transition point from a fragmented to a damaged sheet appears at $\sigma \approx 0.03$. The snapshots of Figs. 1(A) and 1(B) were taken before the fragmentation process was completed. The crack nucleation points and propagating cracks with splitting and branching are clearly visible. Decrease in the density of nucleated cracks when σ is increased to a value closer to that at the transition point is also evident. Figure 1(C) shows the final configuration in a case when damping is considerably increased. A reduction in crack branching is obvious.

Figure 2 shows fragment-size distributions $n(s)$ for disorder type I, with $\sigma=0.018$ in Fig. 2(A) and $\sigma=0.025$ in Fig. 2(B). In these two cases, the damping coefficient is $c=10^{-3}$. This value of c means that crack branches propagate easily and λ becomes large. We have therefore fitted the numerical results by Eq. (3) with $s_0=\lambda^D$. These fits are obviously excellent, especially when one takes into account that λ is the only relevant fitting parameter. To further support the parameter reduction, λ^D/s_0 is plotted in Fig. 2(D) as a function of damping coefficient c. Not very surprisingly, $\lambda^D/s_0 = \exp(-c/\text{constant})$ (the crack branches are formed in the elastic unloading around a crack, which behaves as a damped harmonic oscillator). This justifies the assumption made above that $s_0=\lambda^D$ for small c.

As mentioned above, s_0 is related to the density of the nucleated cracks through $s_0 \propto \rho^{-1}$. At a low enough strain no beams will break, and s_0 diverges. As it is the only relevant parameter for $c \approx 0$, $s_0^{1/D}$ can be considered as a correlation length (i.e., the typical maximum distance between beams that belong to the same fragment). For systems of size $L > s_0^{1/D}$, the scaling of this correlation length can be investigated by fitting the numerical distributions by Eq. (3). Close to the transition point the correlation length becomes bigger than L. Its scaling can then be investigated through the probability $\Pi(\sigma, L)$ that a system of size L is fragmented at fracture threshold σ. The probability distribution of the density of broken bonds is bimodal near the transition point. This distribution can be interpreted so that damaged systems are

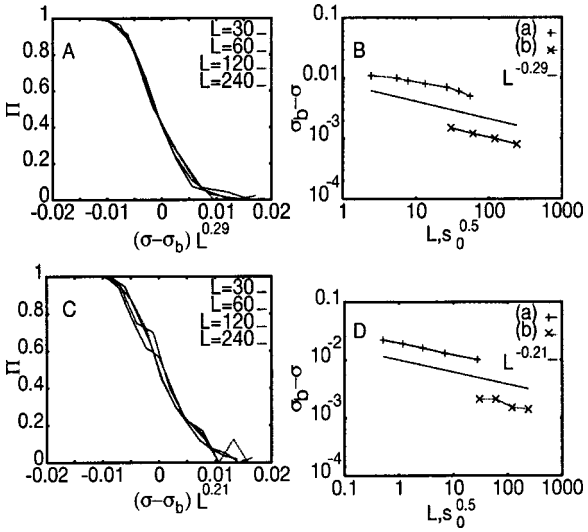

FIG. 3. (**A**) $\hat{\Pi}((\sigma-\sigma_b(L))L^{1/\nu},L)$ for disorder type I. (**B**) $\sigma_b-\sigma$ as a function of $\sqrt{s_0}$ for $L=120$ (a), and the standard deviation of $\Pi(\sigma,L)$ as a function of L (b). Disorder is of type I. (**C**) and (**D**) show the corresponding results for disorder type II.

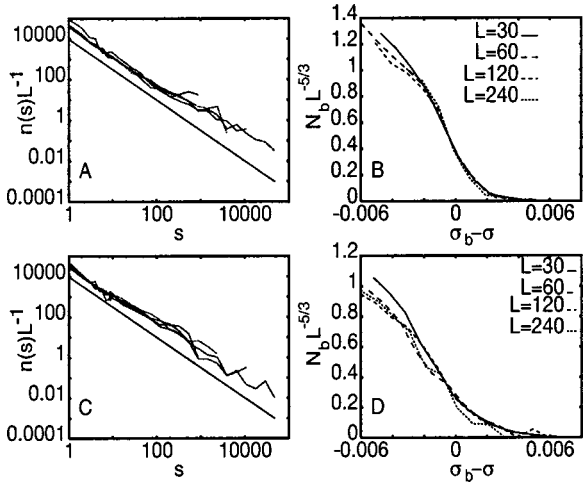

FIG. 4. (**A**) $n(s)L^{-1}$ as a function of s for $L=30,60,120,240$. For comparison the line $s^{-(2D-1)/D}$ is also shown. (**B**) $N_bL^{\beta-D}$ as a function of $\sigma_b-\sigma$. In both (**A**) and (**B**), disorder type I was used while (**C**) and (**D**) show the corresponding results for disorder type II.

those with a low density of broken bonds and fragmented systems are those with a high density. By defining shifted probabilities $\hat{\Pi}(\sigma_s,L)=\Pi(\sigma-\sigma_b(L),L)$ such that $\hat{\Pi}(0,L)=0.5$, we can try data collapse in the form $\hat{\Pi}((\sigma-\sigma_b(L))L^{1/\nu},L)$. This is done in Figs. 3(A) and 3(C) for disorder types I and II, respectively. Here, $\sigma_b(L)$ is the value of σ at which the transition from a damaged to a fragmented state takes place.

Another way of estimating the correlation length is to fit $\Pi(\sigma,L)$ by a Gaussian curve. The standard deviation of the Gaussian fit should scale as $L^{-1/\nu}$. These results together with the results for $\sigma_b-\sigma$ as a function of $\sqrt{s_0}$ are displayed in Figs. 3(B) and 3(D). The main result of Fig. 3 is that the correlation length seems to scale quite nicely, i.e., it appears to diverge as a power law at the transition point, and that the value of the correlation length exponent is about 4, ($\nu=4\pm1.0$). This value is different from that reported in Ref. [3], where $\nu=2/3$ was found. It is thus evident that ν cannot be universal for brittle fragmentation. It is mainly the loading conditions that distinguish the present system from that in Ref. [3], but also disorder should affect ν, at least to some extent.

In order to test the finite-size scaling of the results, $n(s)$ and the total number of broken bonds $N_b(\sigma,L)$ were recorded for different system sizes near the transition point. As predicted above, the fragment-size distributions scale as $n(s)\propto L^{D-1}$ (Fig. 4). The scaling of the largest fragments follow nicely L^2 (this is actually rather trivial). These two scaling laws together are enough to determine that the total surface of fragments scales as L^{D-1}. Now N_b, which is a direct measure of the total fracture surface, can be expected to scale also as L^{D-1}. It is evident from Fig. 4, however, that $N_b\propto L^{5/3}$. The reason for this discrepancy is that only a fraction of the broken bonds are parts of the cracks that form the fragments. If there were only fragment-forming cracks, the number of broken bonds related to a fragment of size L^D would be L^{D-1}. If, in addition to the cracks, there is a substantial amount of broken bonds that never develop into propagating cracks, the number of broken bonds should rather be $\propto L^{D-\beta}$ with $0<\beta<1$. In our case $\beta\approx1/3$. These results were obtained for $c=0.001$ and they demonstrate that in this case the sheets are not far from being completely shattered during fragmentation (complete shattering means $\beta=0$).

V. EXPERIMENTS

For the experiments, 22 disks were each cast by pouring liquid gypsum into a mold and letting it dry for a sufficiently long time to be completely dry. The molded objects were as identical as possible: The diameters of the disks were 10.65 ± 0.10 cm and their heights were 2.28 ± 0.20 cm. In the data analysis, we have treated the disks as identical. The disks were dropped (with zero initial velocity) from a varying height, and they impacted onto a metal plate placed on a concrete floor. In order to collect all the fragments resulting from the impact, the disks were wrapped loosely into a thin cellophane membrane. Above the top surface of the disks, opposite to the impact surface, the remaining cellophane was formed into a tiny parachute (extending up to about 3 cm from the surface of the disk). The purpose of this parachute was to make the disks fall with the flat side down and to evenly impact the floor.

After each impact, we investigated the impact zone to verify that the disk had indeed fallen with its flat side parallel to the floor. The disks were dropped from the heights $h=0.25,0.5,0.75,1,1.5,2,2.5,3,5,7,$ and 10 m. For each height, two disks were used so that totally 22 experiments were done. After each impact, the masses of the fragments were carefully weighed. In the analysis of the data, only masses bigger than 0.1 mg were used, although the masses

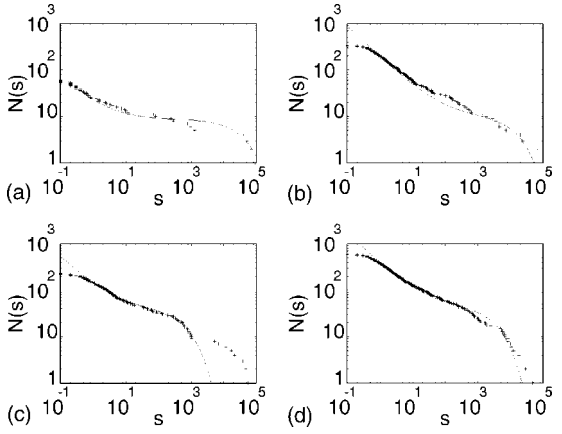

FIG. 5. Fragment-mass distributions $N(s,\lambda,\beta_r)$ obtained for different heights h. In (**A**), $h=0.75$ m, and function $10N(s,75,1.3\times10^{-4})$ is shown as a line. In (**B**), $h=3.0$ m and the line is $130N(s,55,3\times10^{-5})$, in (**C**) $h=7.0$ m and the line is $75N(s,19,5\times10^{-3})$, while in (**D**) $h=10.0$ m and the line is $250N(s,33,3.2\times10^{-4})$. From (**C**), it appears that only one part of the disk has fragmented properly. The rest of it has probably been cleaved into a few large fragments.

of all fragments were measured in order to be fairly sure that all fragments heavier than 0.1 mg were indeed included in the analysis.

In the $h=0.25$ and 0.5 m drops the disks did not break, but higher elevations gave disks impact energy enough for fragmentation. Figure 5 displays the fragment-size distributions for $h=0.75, 3.0, 7.0,$ and 10.0 m. These distributions are compared with the integrated form, $N(s)=\int_s^\infty n(s)ds$, of Eq. (3). There are fairly large variations in the data as the statistics is not very extensive, but comparison with the theoretical distribution is nevertheless decent for about one third of the experiments. For the rest of the drops, the concave shape of the distribution is not clearly visible, and power laws with exponents smaller than the theoretical value provide better fits (in such cases the exponent depends on the impact energy so that exponents closer to the theoretical one are found for larger h). In contrast with this, for the quarry blasting experiments [29], the theoretical value gave a perfect fit.

From Fig. 5, it is also evident that there are large uncertainties in fitting the parameter $s_0=\lambda^D$, and therefore an investigation of its scaling behavior becomes difficult. In order to estimate ν, we fitted the experimental data with Eq. (3) and with function $N(s)\propto s^{-\hat{\beta}}\exp(-s/s_0)$, with $\hat{\beta}$ and s_0 as the adjustable parameters. Figure 6 shows the values obtained for $s_0^{1/3}$ as a function of $\sqrt{h}-\sqrt{h_c}$, with $h_c\approx0.6$. The largest fragment of each experiment is also shown in Fig. 6. These results gave $\nu\approx0.25$, which is a very small value. The uncertainty is however large as is evident from Fig. 6.

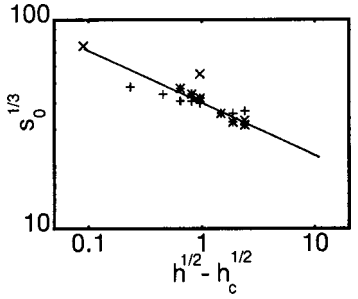

FIG. 6. The linear cutoff fragment size $s_0^{1/3}$ as a function of $\sqrt{h}-\sqrt{h_c}$. The line is $s_0^{1/3}\propto(\sqrt{h}-\sqrt{h_c})^{-0.25}$. The data are obtained from the largest fragments (∗), a fit by Eq. (3) (×), and a fit by $N(s)\propto s^{-\hat{\beta}}\exp(s/s_0)$ (+).

VI. SUMMARY AND DISCUSSION

To summarize, we have given arguments in support of an analytical expression for the fragmentation-size distribution in any dimension D, and shown that this distribution reproduces experimentally observed distributions for a class of brittle fragmentation processes. The arguments used are exact for $D=1$, and the proposed distribution reduces in a realistic limit to the empirical GS distribution for $D=3$. Initially nucleated cracks propagate and develop branches, which mutually merge so as to form an exponential and a scale invariant contribution, respectively, to the fragment-size distribution. The effects of elastic relaxation and dissipation were taken into account by introducing a penetration depth for the side branches.

Numerical data with two types of quenched disorder, and experiments on gypsum disks, were found to agree with the proposed distribution. The density of the initially nucleated cracks was shown to decrease when the transition from a fragmented to a merely damaged state was approached by reducing the impact energy, leading to a divergence in the typical fragment size. This typical fragment size (its linear version) can be considered as a correlation length in the problem. Its divergence can thus be used to determine a correlation length exponent ν. We found that $\nu=4\pm1.0$ for our $D=2$ numerical data, while $\nu=0.25\pm0.05$ for our $D=3$ experimental data. Both values differ from the earlier findings for ν in systems with different loading conditions. We can thus deduce that the scaling of the correlation length appears to be system dependent in fragmentation of brittle materials, which in this respect does not show universality.

Cascade fragmentation can be defined as one in which each fragment goes through a repetitive breakup. If the amount of breakups is an uncorrelated random variable, the result will be a log-normal fragment-size distribution. Power-law fragment-size distributions can also be obtained in cascade fragmentation by defining the amount of breakups as a time variable and a probabilistic stopping criterion for the breakup [30]. Such models are particularly interesting in relation to grinding type of fragmentation, but may also be relevant to instant fragmentation. The fragmentation processes investigated here are such that the final fragment-size distribution is formed essentially in a single breakup event. The fragment-size distribution is in this case a power law, an exponential function, or a combination of the two. The model reported here provides a unified explanation to this qualitative variation in the fragment-size distributions observed in instant fragmentation.

Pure power laws are seldom found in nature; in our model, they appear only when the energy is right at the tran-

sition point from a damaged to a fragmented state, is uniformly distributed over the sample, and the material is fragile enough for branches to propagate without stopping across the sample. Such cases may obviously appear quite unfrequently. More commonly, power-law distributions with exponential large-size cutoffs are encountered. These fragment-size distributions are related to fragmentation that takes place away from the transition point. Still farther away from the transition point the power-law part of the distribution diminishes as the fragments resulting from the Poisson process become smaller. In materials that are not very fragile, we also expect that branches do not propagate very far, and the fragment-size distribution should also in this case become an exponential function, given that the loading conditions are such that crack nucleations are more or less random events. If this is not the case, and the material is not very fragile, we would expect the fragment-size distribution to show little, if any, universality.

[1] J. A. Åström, M. Kellomäki, and J. Timonen, Phys. Rev. E **55**, 4757 (1997).
[2] F. Kun and H. J. Herrmann, Phys. Rev. E **59**, 2623 (1999).
[3] J. A. Åström, B. L. Holian, and J. Timonen, Phys. Rev. Lett. **84**, 3061 (2000).
[4] C. J. Waddington and P. S. Freier, Phys. Rev. C **31**, 888 (1985).
[5] J. E. Finn *et al.*, Phys. Rev. Lett. **49**, 1321 (1982).
[6] W. Bauer, D. R. Dean, U. Mosel, and U. Post, Phys. Lett. **150B**, 53 (1985).
[7] M. Kleine Berkenbusch *et al.*, Phys. Rev. Lett. **88**, 022701 (2002).
[8] J. Bondorf, A. S. Botvina, A. S. Iljinov, I. N. Mishustin, and K. Sneppen, Phys. Rep. **257**, 133 (1995).
[9] R. Schuhmann, Trans. AIME **217**, 22 (1960).
[10] A. M. Gaudin and T. P. Meloy, Trans. Soc. Min. Eng. AIME **223**, 40 (1962).
[11] J. A. Åström and H. J. Herrmann, Eur. Phys. J. B **5**, 551 (1998).
[12] R. T. Chancey, L. Oddershede, F. E. Harris, and J. R. Sabin, Phys. Rev. A **67**, 043203-1 (2003).
[13] L. Oddershede, P. Dimon, and J. Bohr, Phys. Rev. Lett. **71**, 3107 (1993).
[14] R. Ogul and A. S. Botvina, Phys. Rev. C **66**, 051601 (2002).
[15] For recent measurements, see, e.g., E. T. Stamboliadis, Minerals Eng. **15**, 707 (2002); C. Hosten and O. San, Minerals Eng. **15**, 347 (2002).
[16] B. L. Holian and D. E. Grady, Phys. Rev. Lett. **60**, 1355 (1988).
[17] D. E. Grady and M. E. Kipp, J. Appl. Phys. **58**, 1210 (1985).
[18] For a recent review, see, e.g., J. Fineberg and M. Marder, Phys. Rep.0370-1573 313 (1999), and references therein.
[19] H. Inaoka and H. Takayasu, Physica A **229**, 5 (1996).
[20] J. A. Åström and J. Timonen, Phys. Rev. Lett. **78**, 3677 (1997).
[21] Y. Hayakawa, Phys. Rev. B **53**, 14828 (1996).
[22] E. Sharon and J. Fineberg, Phys. Rev. B **54**, 7128 (1996).
[23] J. J. Gilvarry, J. Appl. Phys. **32**, 391 (1961).
[24] A. Meibom and I. Balslev, Phys. Rev. Lett. **76**, 2492 (1996).
[25] H. Inaoka, E. Toyosawa, and H. Takayasu, Phys. Rev. Lett. **78**, 3455 (1997).
[26] T. Kadono and M. Arakawa, Phys. Rev. E **65**, 035107 (2002).
[27] H. Katsuragi, D. Sugino, and H. Honjo, Phys. Rev. E **68**, 046105 (2003).
[28] T. Kadono, Phys. Rev. Lett. **78**, 1444 (1997).
[29] J. A. Åström, F. Ouchterlony, R. P. Linna, and J. Timonen, Phys. Rev. Lett. (to be published).
[30] M. Marsili and Y.-C. Zhang, Phys. Rev. Lett. **77**, 3577 (1996).